
Supplementary information

**Mass spectrometry of short peptides
reveals common features of metazoan
peptidergic neurons**

In the format provided by the
authors and unedited

1 **Supplementary information**

2 **Mass spectrometry of short peptides reveals common features of metazoan peptidergic**
3 **neurons**

4 Eisuke Hayakawa*, Christine Guzman, Osamu Horiguchi, Chihiro Kawano, Akira Shiraishi, Kurato
5 Mohri, Mei Fang Lin, Ryotaro Nakamura, Ryo Nakamura, Erina Kawai, Shinya Komoto, Kei Jokura,
6 Kogiku Shiba, Shuji Shigenobu, Honoo Satake, Kazuo Inaba & Hiroshi Watanabe*

7

8 **1. Supplementary methods**

9 **1.1 Sample preparation for mass spectrometry**

10 **1.2 Mass spectrometry analysis**

11 **1.3 Peptide identification**

12 **1.4 Cleavage site analysis**

13 **1.5 Homology analysis for peptide precursors**

14 **1.6 Antibody validation**

15 **1.7 siRNA-mediated knockdown of neuropeptides in *N. vectensis* embryos**

16 **1.8 Quantitative reverse transcription polymerase chain reaction (qPCR)**

17 **1.9 Reproducibility of microscopic data**

18

19 **2. Supplementary figures**

20 **2.1 Supplementary Figure 1**

21 **2.2 Supplementary Figure 2**

22 **2.3 Supplementary Figure 3**

23 **2.4 Supplementary Figure 4**

24 **2.5 Supplementary Figure 5**

25 **2.6 Supplementary Figure 6**

26 **2.7 Supplementary Figure 7**

27 **2.8 Supplementary Figure 8**

28

29

30

31

32 **1. Supplementary methods**

33 **1.1 Sample preparation for mass spectrometry**

34 *For Nematostella vectensis*, six young adult polyps (about 10 mm in length) were mixed with 4 ml of
35 acidified methanol solution (90% methanol, 9% ultrapure water, and 1% formic acid) together with
36 zirconia beads (2.0 mm diameter) and immediately subjected to homogenization. For *Ephydatia*

37 *fluviatilis*, ten animals (about 10 mm diameters) were mixed with 4 ml of acidified methanol together
38 with the same zirconia beads and immediately subjected to homogenization. For *Bolinopsis mikado*,
39 immediately before extraction, three animals were cut into small pieces, then a large part of the
40 mesoglea was removed with a surgical knife. The remaining tissue was mixed with 4 ml of acidified
41 methanol together with the same zirconia beads and immediately subjected to homogenization.
42 Homogenizations were performed with a bead homogenizer (Bead Smash 12, Waken B Tech) for
43 three cycles at 3,000 rpm for 30 sec at 4 °C with an intermediate 30-sec pause. After
44 homogenization, debris and large proteins were removed from the samples by centrifugation (4 °C at
45 13,000 g for 20 min). The supernatant was first vacuum dried with GeneVac EZ-2 Elite (SP
46 Scientific) and then resuspended in 500 µl of 1% methanol with 0.5% formic acid, then subjected to
47 the solid phase extraction. Oasis HLB 1 cc cartridge (30 mg, Waters) was used for solid-phase
48 extraction together with vacuum manifold (Extraction Manifold, Waters). The cartridges were first
49 activated with 1 ml of solvent B (70% acetonitrile with 0.1% formic acid), followed by equilibration
50 with 1 ml of solvent A (1% acetonitrile with 0.1% formic acid). Resuspended samples were loaded
51 onto the cartridges and washed with 1 ml of solvent A. The bound peptides were eluted with 1 ml of
52 solvent B. The eluents were dried with GeneVac EZ-2 Elite and stored at -80 °C until LC-MS/MS
53 analysis. This sample preparation procedure was performed independently four times for each
54 animal and the resultants were subjected to the following analysis separately. One of the four
55 extracted replicates was subjected to fractionation to reduce sample complexity before LC-MS/MS
56 analysis. Fractionation was performed according to high-pH RP protocol¹ with slight modification.
57 Dionex UltiMate 3000 HPLC system (Thermo Fischer Scientific) was used for fractionation together
58 with XBridge Peptide BEH C18 Column (2.1 x 100 mm, 3.5 µm particles, 300 Å pores). Mobile phase
59 A is 5 mM ammonium hydroxide (pH 10) and B is 90% acetonitrile, 5 mM ammonium hydroxide (pH
60 10). The flow rate was set to 0.2 ml min⁻¹ and the column temperature was maintained at 40 °C
61 during the runs. The samples were fractionated with a 53 min gradient as follows: 1% B in 3 min, 1-
62 25% B in 27 min, 25-40% B in 13 min, 40-80% B in 5 min, 80% B in 5 min. Fractions were made for
63 every 50 sec, resulting in a total of 72 fractions. The fractions were then pooled and concatenated
64 with other fractions to create 12 combined fractions as described by Wang *et al.*². The fractions
65 were dried with GeneVac EZ-2 Elite and stored at -80 °C until LC-MS/MS analysis.

66

67 **1.2 Mass spectrometry analysis**

68 Three non-fractionated samples and pooled fractionated samples from each animal were analyzed
69 by means of the LC-MS/MS analysis as follows. Dried samples were resuspended in 35 µL of
70 resuspension solution (5% methanol with 0.1% formic acid) with iRT peptides (Biognosys). Fusion
71 Lumos (Thermo Fisher Scientific) coupled with nano-flow liquid chromatography (nanoACQUITY,
72 Waters) was used for LC-MS/MS analysis. The samples were loaded by auto-sampler into a trap

73 column (nanoACQUITY UPLC 2G-V/M Trap 5 μ m Symmetry C18, 180 μ m x 20 mm, Waters) and
74 subsequently an analytical column (nanoACQUITY UPLC HSS T3 1.8 μ m, 75 μ m x 150 mm). Mobile
75 phase A is 0.1% formic acid in water and B is 0.1% formic acid in 80% acetonitrile. The flow rate was
76 set to 500 nl min⁻¹ and the column temperature was maintained at 40 °C during the runs. The
77 samples were separated with a 65 min gradient as follows: 1-7% B in 1 min, 7-13% B in 1 min, 13-
78 50% B in 38 min, 50-99% B in 1 min, 99% B in 9 min, 99-1% B in 1 min and 1% B in 14 min. The
79 eluent was ionized by electrospray ionization with the following setting (RF lens: 30%; spray voltage:
80 2020 V at 0 min, 2020 V at 30 min, 2400 V at 40 min, 2800 V at 50 min, 2020 V at 55 min; sheath
81 gas: 16; auxiliary gas: 2; ion transfer tube temperature: 305 °C). Fragment ion spectra of peptides
82 were acquired in data-dependent acquisition approach using CHarge Ordered Parallel Ion aNalysis³
83 with slight modification. Precursor ions were analyzed in the Orbitrap (AGC target 4 x 10⁵, 50 ms
84 maximum injection time, 120,000 mass resolution). For every survey scan, the top 10 most intense
85 peptide ions were selected for fragmentation at a normalized collision energy of 25% (HCD) or 28%
86 (CID) based on their intensities and their fragment ion spectra acquired in the ion trap detector. Our
87 aim was to perform systematic peptide identifications for three target animals with similar analytical
88 conditions. To this end, prior to the main LC-MS/MS analysis for peptide identifications, we first
89 performed an analysis to acquire signal abundances of each sample. The relative signal abundance
90 of samples is estimated based on the total ion current of each LC-MS run. The loading volume is
91 adjusted so each injection has roughly similar amounts, as well as ion current in the LC-M/MS
92 analysis.

93

94 **1.3 Peptide identification**

95 Peptide-to-spectrum matching was performed using PEAKS X software (PEAKS Studio version
96 10.0, Bioinformatics Solutions) and Mascot (version 2.7, Matrix Science). For PEAKS X, the raw
97 data recorded with Xcalibur (version 4.5, Thermo Fisher Scientific) were directly used. The raw data
98 of the acquired MS/MS spectra were processed with PEAKS X software (Bioinformatics Solutions).
99 PEAKS DB algorithms were utilized to perform peptide-to-spectrum matchings. The search
100 parameters are as follows: 3 ppm for precursor tolerance, 0.3 Da for fragment tolerance, and no
101 fixed modifications. Variable modifications were oxidation of Methionine (15.99491 Da),
102 pyroglutamation from Glutamic acid (-18.01057 Da) or Glutamine (-17.02655Da), and amidation at
103 peptide C-termini (-0.98402 Da) for PEAKSDB or Glycine-loss amide (-58.005479) for Mascot. For
104 Mascot, fragment ion spectra were extracted in mgf file format from the raw format using MS convert
105 in ProteoWizard package⁴ 3.0.20139. The same search parameters for mass tolerance and variable
106 PTM were used for Mascot as well. Searches were performed against amino acid sequences
107 translated in six frames from the transcriptome data of the respective animal species. Transcriptome
108 sequence data for *B. Mikado* (Yokohama, Kanagawa) was prepared as described in the main

109 manuscript and data sets of other species were acquired from public data set⁵⁻⁷. It is known that
110 extracted peptide fractions may contain naturally occurring protein fragments as well as protein
111 degradation products caused during the sample processing, which are not relevant to
112 neuropeptides. In order to remove such peptides from the peptide-to-spectrum matching result, the
113 following filtering process was performed. HMMER⁸ (version 3.2.1) was used to scan precursor
114 proteins of detected peptides for Pfam⁹ motifs version 33.1. All peptides whose precursor protein
115 included any Pfam motifs except for neuropeptide-related motifs
116 (PF05874,PF11109,PF14993,PF15085,PF15180,PF08257,PF15161,PF05953,PF01160,PF04736,P
117 F08111,PF15171,PF02323,PF03858,PF05824,PF08035,PF08258,PF08259,PF08260,PF17308,PF0
118 0123,PF01581,PF07421,PF02202,PF11105,PF02044,PF08187,PF00473,PF00918,PF01147,PF030
119 02) with an e-value cutoff of 1e-10 were removed and not processed in the following analysis.
120 In this study, we focus on naturally occurring peptides with C-terminal amidation as neuropeptide
121 candidates. To this end, only peptides detected as C-terminally amidated forms were selected and
122 further analyzed. Validation of peptide identification was performed as follows. We consider proteins
123 that produce C-terminally amidated peptide predicted with peptide-to-spectrum matching as tentative
124 peptide precursors. Since we had a large number of peptide candidates, we select one of peptides
125 derived from each precursor proteins as representative and their AA sequences were chemically
126 synthesized. For *N. vectensis*, peptides that show the same structure or derived from previously
127 identified neuropeptide precursors¹⁰ were considered as valid identification, and peptides from novel
128 precursors were selected for peptide synthesis. Peptide synthesis (>80% purity) was performed
129 using ResPep SL (intavis). The synthesized peptides were subjected to LC-MS/MS analysis using
130 the same settings as described above. Fragment ion spectra acquired from the synthetic peptides
131 were manually inspected and compared to the spectra of endogenously detected peptides. The
132 criteria are (1) the presence of the same product ions used for peptide-spectrum matching and (2)
133 relative intensities of the matched ions. If a representative peptide was validated with synthesized
134 peptides, other peptide-to-spectrum matching results derived from the same precursor protein were
135 also considered valid. The raw LC-MS/MS data sets, the output of peptide-to-spectrum matching, six
136 frame-translated AA sequence data sets used, the result of Pfam motif scan, the list of synthetic
137 peptides, and the result of validation with synthetic peptides have been deposited to the
138 ProteomeXchange Consortium with the data set identifier PXD030145
139 (<https://repository.jpostdb.org/preview/194169514461ab01a6d09da>, Access key : 1700).

140

141 **1.4 Cleavage site analysis**

142 Lists of endogenous peptides of, *Drosophila melanogaster*, *Lineus longissimus*, and *Homo sapiens*
143 were acquired from the studies of mass spectrometry-based peptide identifications¹¹⁻¹³. When length
144 variants were found in the list of peptides, only the longest forms were used to annotate cleavage

145 sites to avoid endogenous or artificial degradation products. AA composition of N and C-terminal
146 cleavage sites (2 AA, excluding Glycine for amide donor) of peptides were counted for each data
147 set. For WebLogo representation, N and C-terminal flanking regions of 6 AA were collected from the
148 data sets. In case the length of N or C-terminal flanking regions was less than 6 AA, such regions
149 were excluded.

150

151 **1.5 Homology analysis for Neuropeptide precursors**

152 Sequence data of Ctenophora species (*Beroe abyssicola*, *Beroe sp.*, *Bolinopsis ashleyi*, *Bolinopsis*
153 *infundibulum*, *Coeloplana astericola*, *Dryodora glandiformis*, *Euplokamis dunlapae*, *Mertensiidae sp.*,
154 *Mnemiopsis leidyi*, *Pukia falcata*, *Vallicula multiformis*) were acquired from Neurobase
155 (<https://neurobase.rc.ufl.edu/>). Homologs of *B. mikado* neuropeptide precursors were searched
156 against the sequences data by performing a local tblastn search (version 2.11.0+)¹⁴. Homologs of *N.*
157 *vectensis* neuropeptide homologs were acquired by searching against NCBI transcriptome Shotgun
158 Assembly of Cnidarian species using an online tblastn interface. Blast search results were manually
159 validated based on the criteria (1) the presence of mature neuropeptide structurally related to the
160 identified peptides of *N.*, *vectensis*, or *B. mikado* and (2) the presence of Glycine at the C-terminal
161 flanking region as amide donor. AA sequences of other neuropeptide precursors were acquired from
162 Jekeley¹⁵ and Thiel *et al.*¹⁶. The sequences of neuropeptide precursors were assembled
163 (Supplementary data 4) and subjected to an all-against-all Basic Local Alignment Search Tool
164 (BLAST) search (blastp, version 2.11.0+)¹⁴. Clustering and visualization were performed on
165 Cytoscape software (version 3.5.1)¹⁷ with an e-value cutoff of 1e-5.

166

167 **1.6 Antibody validation**

168 Validation of the primary antibodies against NPWa and VWY_a was performed by negative control
169 immunostaining for *B. mikado* and *V. multifomis*, respectively. The basic procedure of
170 immunostaining was the same as the method section of the main manuscript., but negative control
171 samples were incubated in blocking solution without the primary antibodies. Images of the negative
172 control samples were recorded with the same laser intensity and exposure time. The recording was
173 performed by the Olympus SD-OSR confocal microscopy (Supplementary Figure 6, 7).

174

175 **1.7 siRNA-mediated knockdown of neuropeptides in *N. vectensis* embryos**

176 In order to check the specificity of each antibody, we performed small interference RNA (siRNA)-
177 mediated gene knockdown of neuropeptide precursor mRNAs, followed by immunostaining of
178 neuropeptides. For this purpose, we examined at least four distinct siRNA sequences for each
179 peptide gene and found siRNAs strongly (> 90%) disrupting the RFamide, PRGamide, and
180 QWamide mRNAs (Supplementary Figure 8). We were not able to find the effective siRNA sequence

181 for HIRamide and therefore excluded this peptide from analysis. For knocking down neuropeptides
182 of *N. vectensis*, siRNAs were electroporated to the fertilized eggs as described¹⁹ with following
183 modifications: Eggs were suspended in brackish water (1/3 artificial sea water) with 6% Ficoll. The
184 eggs were electroporated with siRNAs for control (siCtr: 5'-GCAACACGCAGAGUCGUAAdTdT-3'),
185 *NvRFamide* (siRFa: 5'-GCUUGGAAUCCUAAUUCAAAdTdT-3'), *NvPRGamide* (siPRGa: 5'-
186 GAUGAAGAAUCUUUACUUGdTdT-3'), *NvQWamide* (siQWa: 5'-
187 GAAAUUCCGCCACAAGGUUdTdT-3') at 100 ng/μl concentration. Planula larvae were collected for
188 RNA extraction and immunostaining at 4 dpf. Knockdown efficiencies were assessed with qPCR
189 analyses for each experiment.

190

191 **1.8 Quantitative reverse transcription polymerase chain reaction (qPCR)**

192 RT-qPCR was performed on the StepOne Plus™ Real-Time PCR System (Thermo Fisher Scientific)
193 using PowerUp SYBR® Green Master Mix (Thermo Fisher Scientific). The expression levels of
194 analyzed genes were normalized to *Ef1a* and *Gapdh* using $\Delta\Delta C_t$ method. The primers sequences
195 are listed in Supplementary Table 9.

196

197 **1.9 Reproducibility of microscopic data**

198 **Figure 2**

199 a: n=16, b: n=7, c: n=21, d: n=7, e: n=3, f: n=13, g: n=22, h: n=7, i: n=15, j: n=15, k: n=8, l: n=19, m:
200 n=6, n: n=13, o: n=7, p: n=3, q: n=18, r: n=3, s: n=11, t: n=3, u: n=15, v: n=7, w: n=5

201 **Extended Figure 3**

202 a whole body: RFa: n=8, RPGa: n=10, QWa: n=7, HIRa: n=9, sensory: RFa: n=8, RPGa: n=7, QWa:
203 n=6, HIRa: n=9, multipolar: RFa: n=8, RPGa: n=10, QWa: n=7, HIRa: n=9

204 b whole body: RFa: n=5, RPGa: n=8, QWa: n=9, HIRa: n=8, neuroendocrine: RFa: n=5, RPGa: n=8,
205 QWa: n=9, HIRa: n=8

206 **Extended Figure 4**

207 b, c: n=19, d: n=19, e: n=3, f, g: n=6, h: n=4, i, j: n=4, k: n=4, l: n=2, m: n=4, n, o: n=5, p, q: n=4

208 **Supplementary Figure 6**

209 a: n=8, b: n=2

210 **Supplementary Figure 7**

211 a: n=4, b: n=4, c: n=4, d: n=4

212

213

214

215

216 **References**

- 217 1 Batth, T. S., Francavilla, C. & Olsen, J. V. Off-line high-pH reversed-phase fractionation for
218 in-depth phosphoproteomics. *J Proteome Res* **13**, 6176-6186, doi:10.1021/pr500893m
219 (2014).
- 220 2 Wang, Y. *et al.* Reversed-phase chromatography with multiple fraction concatenation
221 strategy for proteome profiling of human MCF10A cells. *Proteomics* **11**, 2019-2026,
222 doi:10.1002/pmic.201000722 (2011).
- 223 3 Davis, S. *et al.* Expanding Proteome Coverage with CHarge Ordered Parallel Ion aNalysis
224 (CHOPIN) Combined with Broad Specificity Proteolysis. *J Proteome Res* **16**, 1288-1299,
225 doi:10.1021/acs.jproteome.6b00915 (2017).
- 226 4 Kessner, D., Chambers, M., Burke, R., Agus, D. & Mallick, P. ProteoWizard: open source
227 software for rapid proteomics tools development. *Bioinformatics* **24**, 2534-2536,
228 doi:10.1093/bioinformatics/btn323 (2008).
- 229 5 Alie, A. *et al.* The ancestral gene repertoire of animal stem cells. *Proc Natl Acad Sci U S A*
230 **112**, E7093-7100, doi:10.1073/pnas.1514789112 (2015).
- 231 6 Tulin, S., Aguiar, D., Istrail, S. & Smith, J. A quantitative reference transcriptome for
232 *Nematostella vectensis* early embryonic development: a pipeline for de novo assembly in
233 emerging model systems. *Evodevo* **4**, 16, doi:10.1186/2041-9139-4-16 (2013).
- 234 7 Sullivan, J. C. *et al.* StellaBase: the *Nematostella vectensis* Genomics Database. *Nucleic*
235 *Acids Res* **34**, D495-499, doi:10.1093/nar/gkj020 (2006).
- 236 8 Finn, R. D., Clements, J. & Eddy, S. R. HMMER web server: interactive sequence similarity
237 searching. *Nucleic Acids Res* **39**, W29-37, doi:10.1093/nar/gkr367 (2011).
- 238 9 El-Gebali, S. *et al.* The Pfam protein families database in 2019. *Nucleic Acids Res* **47**, D427-
239 D432, doi:10.1093/nar/gky995 (2019).
- 240 10 Hayakawa, E. *et al.* A combined strategy of neuropeptide prediction and tandem mass
241 spectrometry identifies evolutionarily conserved ancient neuropeptides in the sea anemone
242 *Nematostella vectensis*. *PLoS One* **14**, e0215185, doi:10.1371/journal.pone.0215185 (2019).
- 243 11 Thiel, D. *et al.* Nemertean, Brachiopod, and Phoronid Neuropeptidomics Reveals Ancestral
244 Spiralian Signaling Systems. *Molecular Biology and Evolution* **38**, 4847-4866,
245 doi:10.1093/molbev/msab211 (2021).
- 246 12 Wegener, C., Reinl, T., Jansch, L. & Predel, R. Direct mass spectrometric peptide profiling
247 and fragmentation of larval peptide hormone release sites in *Drosophila melanogaster*
248 reveals tagma-specific peptide expression and differential processing. *J Neurochem* **96**,
249 1362-1374, doi:10.1111/j.1471-4159.2005.03634.x (2006).

- 250 13 Hook, V. & Bandeira, N. Neuropeptidomics Mass Spectrometry Reveals Signaling Networks
251 Generated by Distinct Protease Pathways in Human Systems. *J Am Soc Mass Spectrom* **26**,
252 1970-1980, doi:10.1007/s13361-015-1251-6 (2015).
- 253 14 Altschul, S. F., Gish, W., Miller, W., Myers, E. W. & Lipman, D. J. Basic local alignment
254 search tool. *J Mol Biol* **215**, 403-410, doi:10.1016/S0022-2836(05)80360-2 (1990).
- 255 15 Jekely, G. Global view of the evolution and diversity of metazoan neuropeptide signaling.
256 *Proc Natl Acad Sci U S A* **110**, 8702-8707, doi:10.1073/pnas.1221833110 (2013).
- 257 16 Thiel, D., Franz-Wachtel, M., Aguilera, F., Hejnol, A. & Wray, G. Xenacoelomorph
258 Neuropeptidomes Reveal a Major Expansion of Neuropeptide Systems during Early
259 Bilaterian Evolution. *Molecular Biology and Evolution* **35**, 2528-2543,
260 doi:10.1093/molbev/msy160 (2018).
- 261 17 Lopes, C. T. *et al.* Cytoscape Web: an interactive web-based network browser.
262 *Bioinformatics* **26**, 2347-2348, doi:10.1093/bioinformatics/btq430 (2010).
- 263 18 Pang, K. & Martindale, M. Q. Developmental expression of homeobox genes in the
264 ctenophore *Mnemiopsis leidyi*. *Dev Genes Evol* **218**, 307-319, doi:10.1007/s00427-008-
265 0222-3 (2008).
- 266 19 Masuda-Ozawa, T. *et al.* siRNA-mediated gene knockdown via electroporation in hydrozoan
267 jellyfish embryos. *bioRxiv*, doi:10.1101/2022.03.24.485716 (2022).
- 268 20 Sebe-Pedros, A. *et al.* Early metazoan cell type diversity and the evolution of multicellular
269 gene regulation. *Nat Ecol Evol* **2**, 1176-1188, doi:10.1038/s41559-018-0575-6 (2018).

270

271

272

273

274

275

276

277

278

279

280

281

282

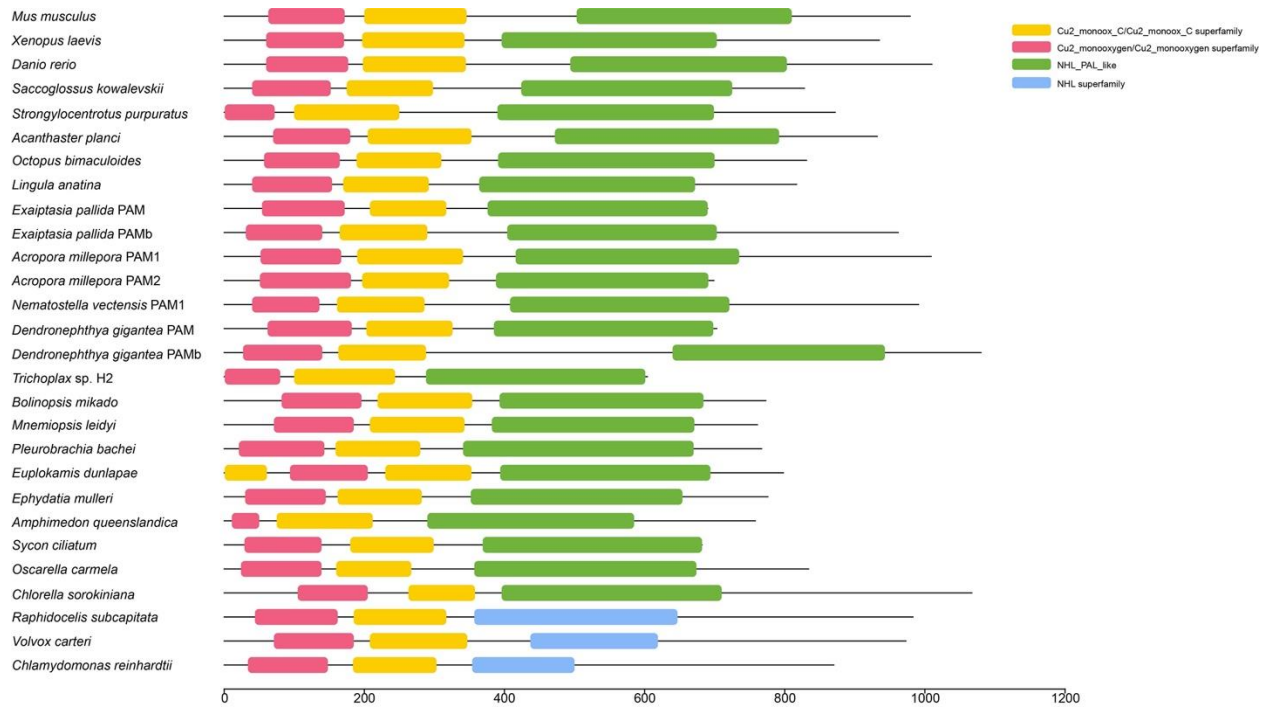
283

284

285 **2 Supplementary Figures**

286

287



288

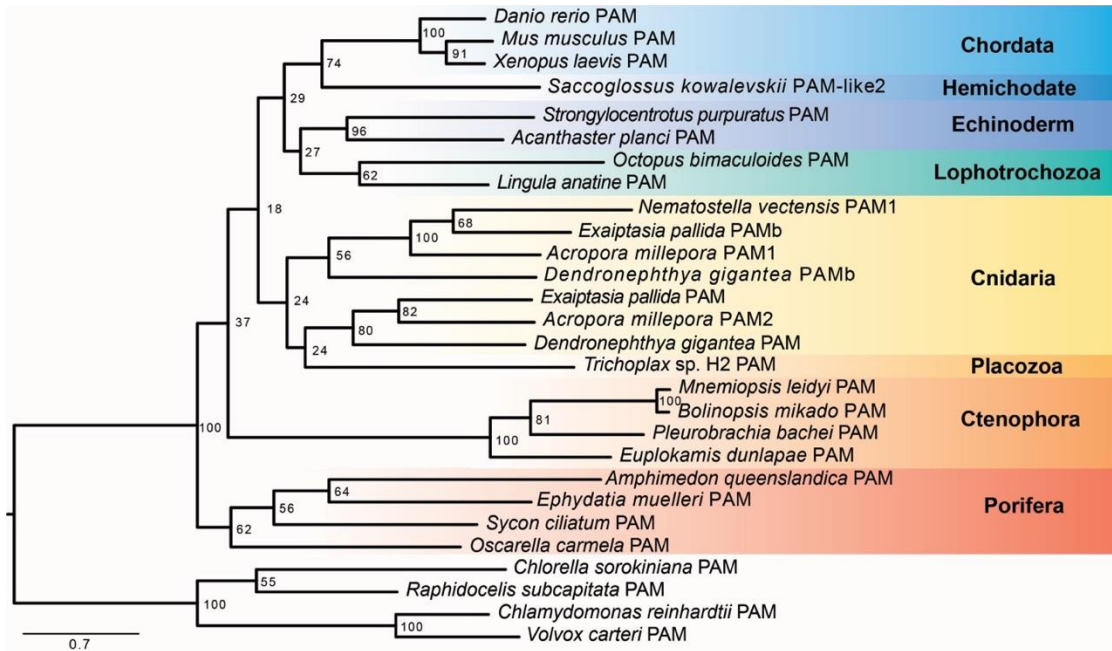
289 **Supplementary Figure 1:** Structure of the PAM genes with predicted functional domains. The
290 schematics showed the identified PAM genes from representative species in Metazoa and unicellular
291 organisms by NCBI conserved domain search interface and HMMER search against Pfam database
292 v.35.0. The scale at the bottom indicates the length (number of residues) of sequences.

293

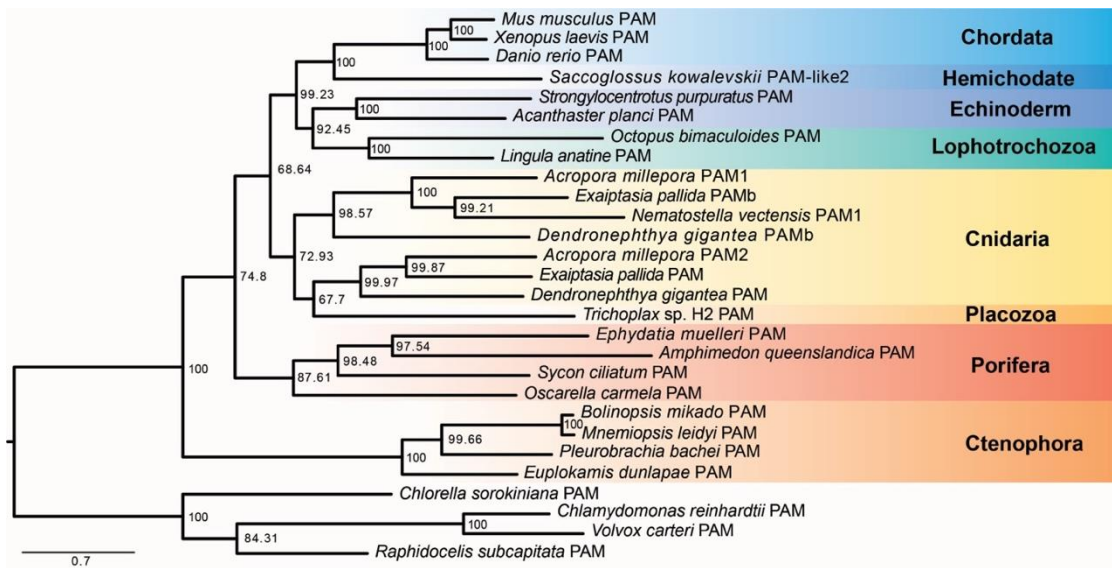
294

295

296

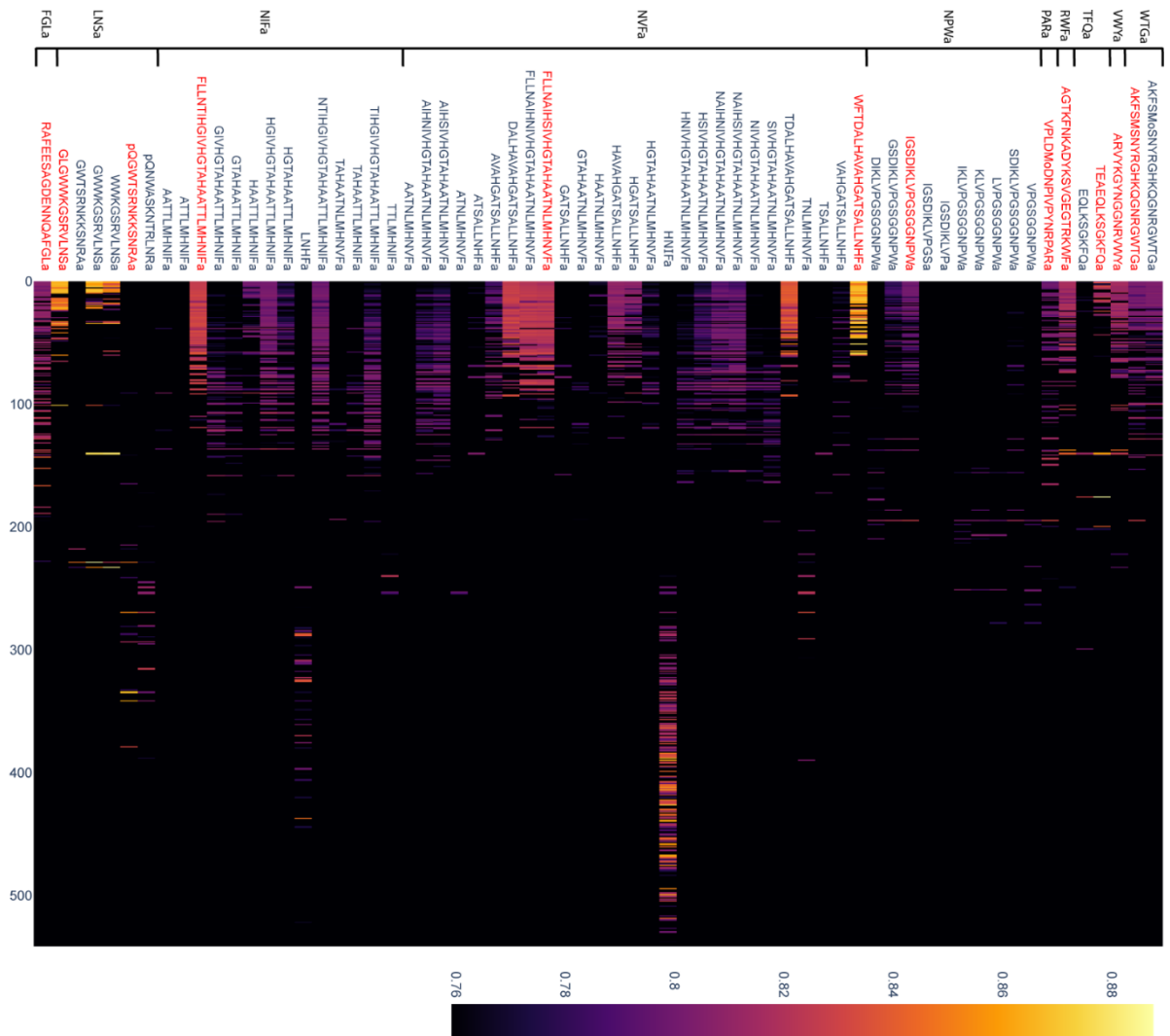


297



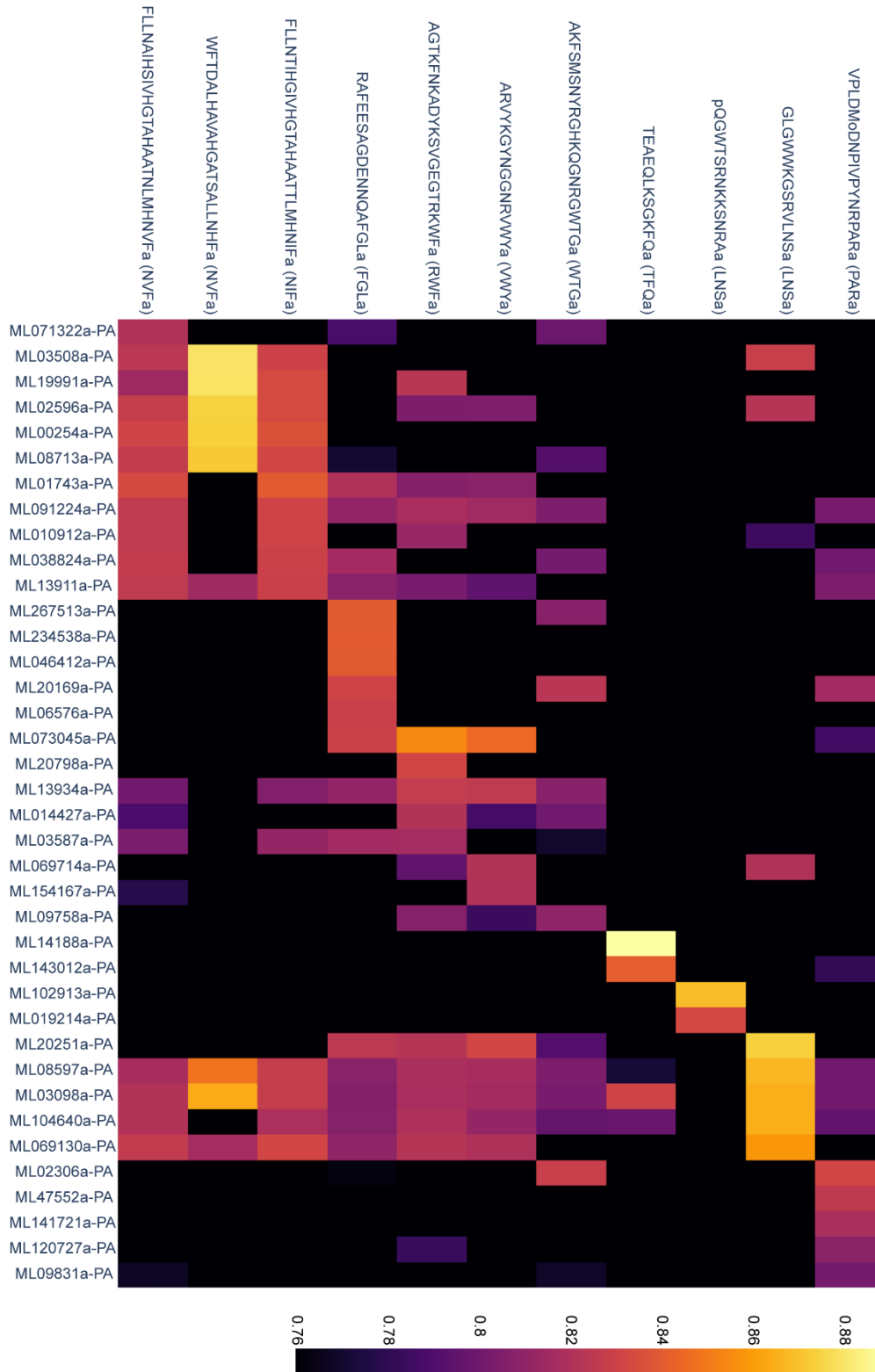
298

299 **Supplementary Figure 2:** Phylogenetic trees of PAM genes. Top: Maximum Likelihood tree,
 300 Bottom; Bayesian tree. The topologies were reconstructed under the WAG+I+G+F amino acid
 301 substitution model. Branching values shown represent the percentage of bootstrap supports under
 302 Maximum Likelihood analysis calculated in PhyML (top) and posterior probabilities under Bayesian
 303 inference implemented in MrBayes (bottom), respectively.

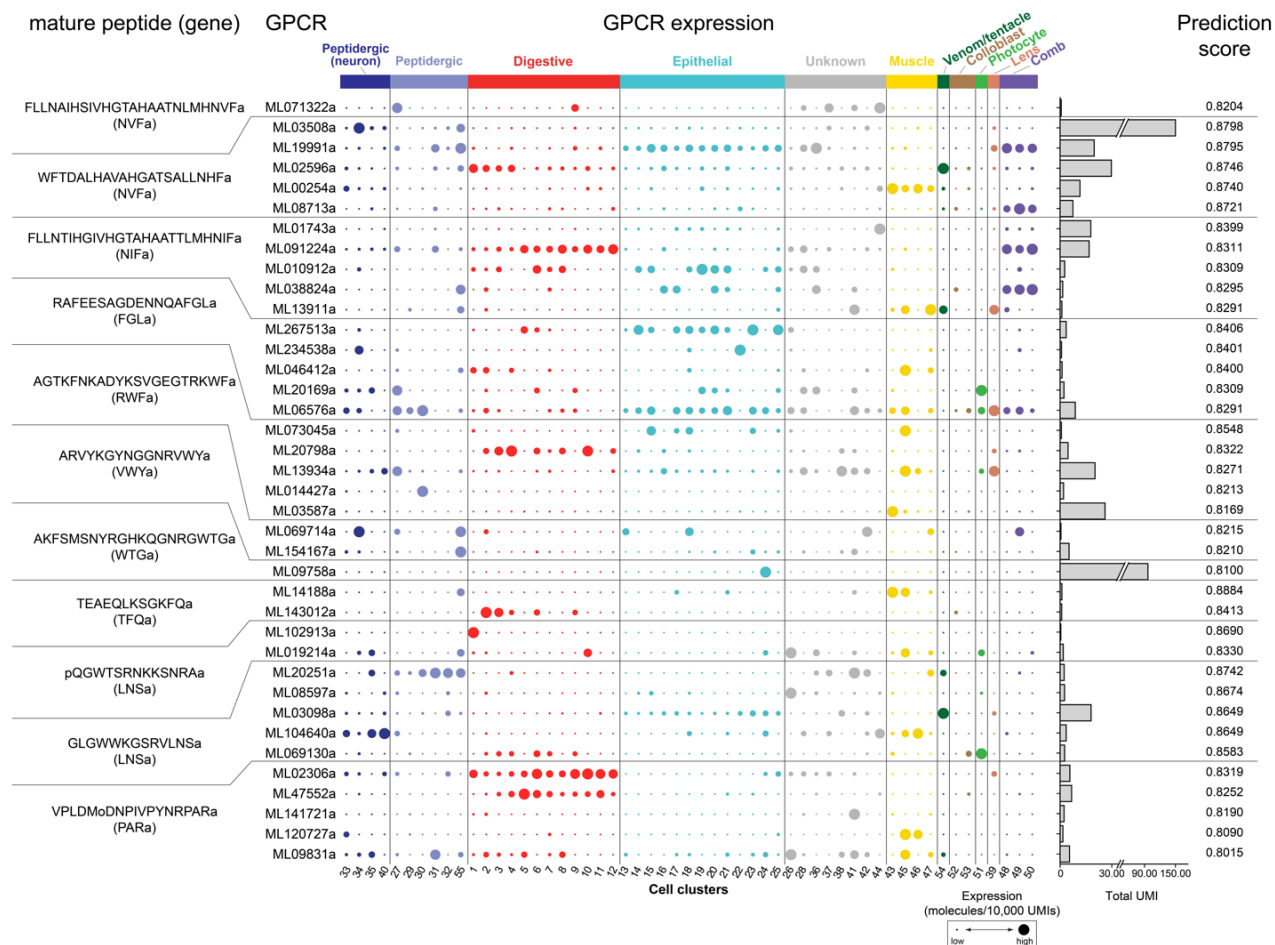


304
 305 **Supplementary Figure 3:** Heatmap representation of peptide-GPCR pair prediction for all *M. leidy*
 306 peptide homologs and GPCRs. Representative peptides for each gene were highlighted in red. Y-
 307 axis shows the indexes of GPCRs in the original result table (Supplementary Table 3). The order of
 308 the Y-axis was sorted by the summation of the scores.

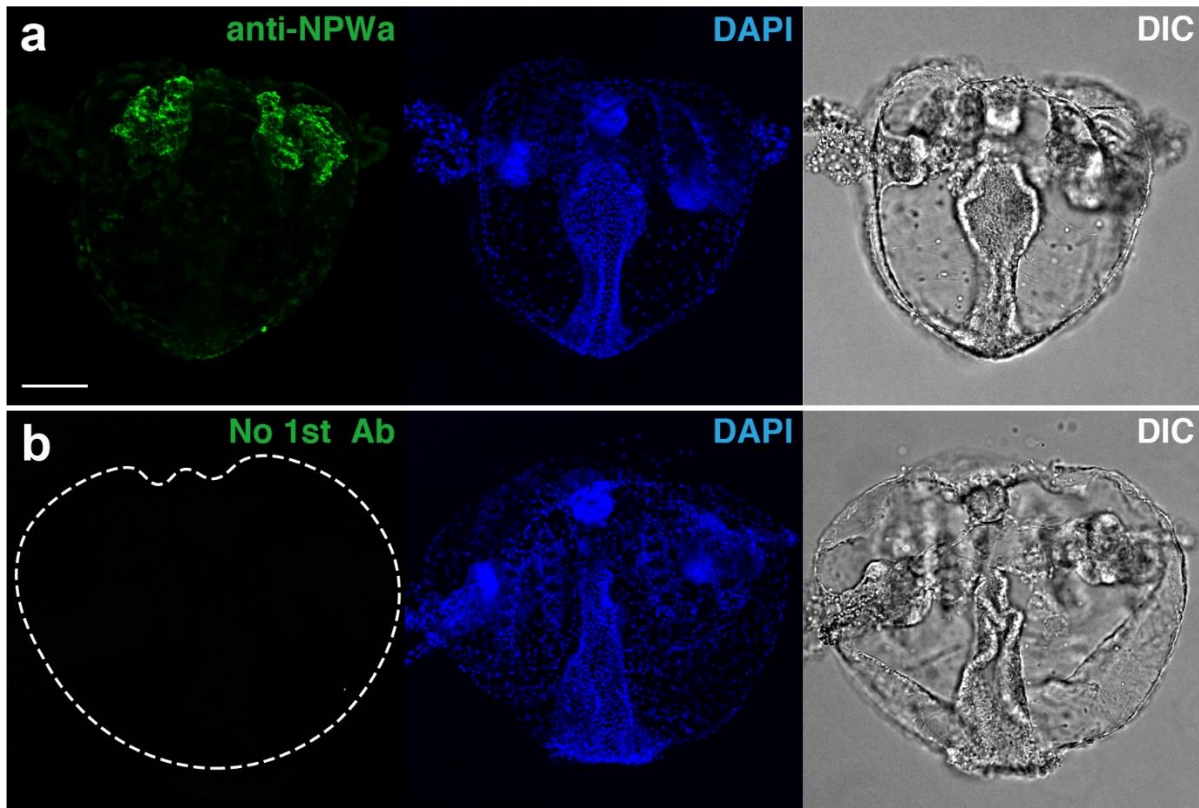
309
310
311
312
313
314
315
316
317
318
319
320
321
322
323
324
325
326
327



Supplementary Figure 4: Heatmap representation of peptide-GCPR pair prediction results shown in Figure 4f.



328
 329 **Supplementary Figure 5: Cell-cluster distribution of putative peptide GPCR receptor expression.**
 330 The representative peptide sequences from each peptide gene (in parentheses) in *M. leidy*
 331 are shown on the left. The dot plot shows the normalized expression values (molecules/10,000 UMIs) of
 332 each GPCR gene across the different cell clusters of adult *M. leidy* scRNA-seq data²⁰. The
 333 expressions are scaled by gene with dot size scales from smallest to largest, corresponding to
 334 lowest and highest expression, respectively. The bar plot shows the actual UMI values. The
 335 communication scores of each peptide-GPCR pair from the prediction model are indicated.
 336
 337
 338



339

340 **Supplementary Figure 6:** Neuropeptide (NPW_a) staining of *B. mikado* with or without the primary
341 antibody. The images of immunostaining performed with (a) or without (b) anti-NPW_a primary
342 antibody. Neuropeptide (green), DAPI (blue), and DIC (bright field). The scale bar, 50 μm.

343

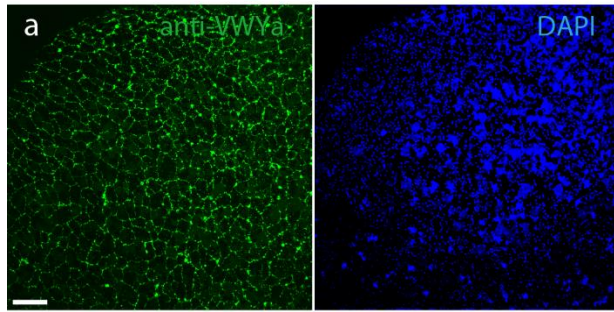
344

345

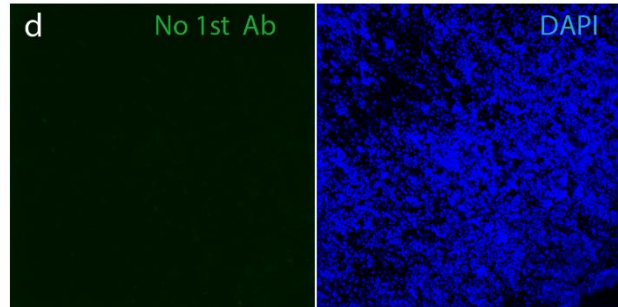
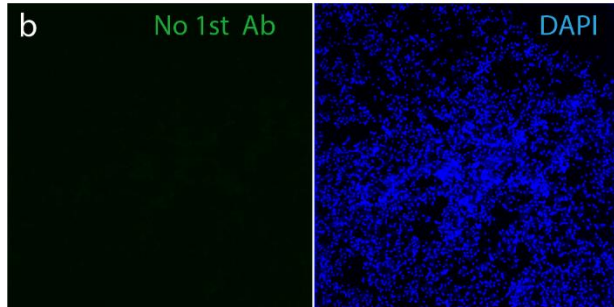
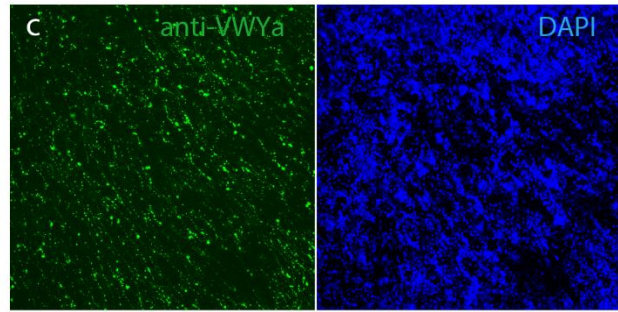
346

347

aboral surface



oral surface



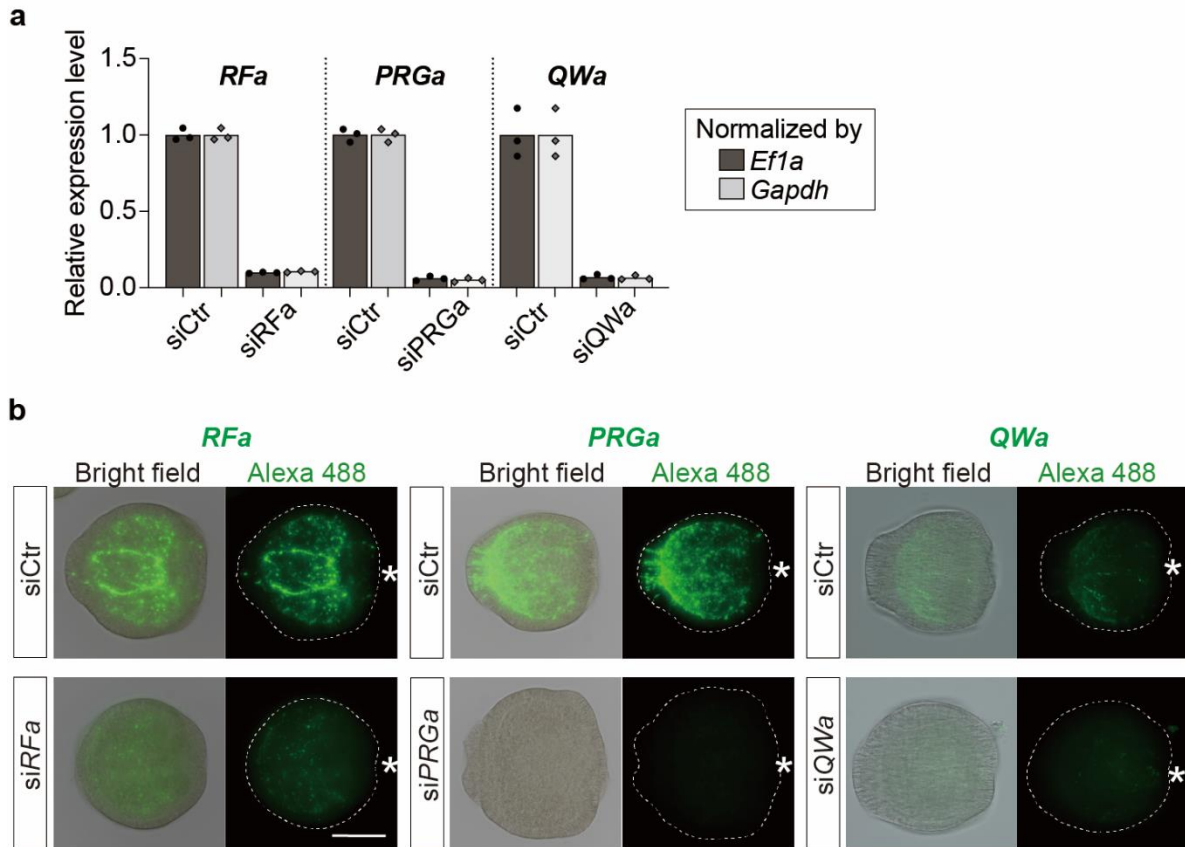
348

349 **Supplementary Figure 7:** Neuropeptide (VWYα) staining of *V. multiformis* with or without the
350 primary antibody. Immunofluorescent staining was performed with (a, c) or without (b, d) anti-VWYα
351 primary antibody. The images of a, b and c, d show aboral and oral surfaces, respectively. The
352 images of Alexa488 (green) and DAPI (blue) fluorescence of the same view were indicated in each
353 panel. Scale bar, 50 μm.

354

355

356



357

358 **Supplementary Figure 8:** siRNA-mediated neuropeptide gene knockdown demonstrates the
 359 antibody specificity of *N. vectensis* neuropeptides. **a**, qPCR data shows the relative expression level
 360 of neuropeptide mRNAs in 4dpf larvae transfected with siRNA for *RFamide*, *PRGamide*, or
 361 *QWamide* precursor mRNAs. Control siRNA (siCtr)-transfected samples were used as the control.
 362 The expression ratio normalized by *Ef1a* and *Gapdh* are indicated as dark and light grey bars,
 363 respectively. The data shown are from a single experiment and representative of at least two
 364 experiments with similar results.

365 **b**, Immunostaining of *RFamide*, *PRGamide* and *QWamide* neuropeptides in control siRNA-
 366 transfected (upper panels) or neuropeptide-specific siRNA-transfected (lower panels) larvae.
 367 Asterisk indicates the oral side. The scale bar, 100 μ m.